Preprint – Whitepaper

This is a non-peer-reviewed preprint submitted to EarthArXiv.

PIKART Version 1.1: Release Notes

S. M. Vallejo-Bernal[1,2], T. Braun[1,2], N. Marwan[1,3], J. Kurths[1]

[1] Research Department Complexity Science, Potsdam Institute for Climate Impact Research (PIK), Member of the Leibniz Association, Potsdam, Germany

[2] Institutefor Earth System Science & Remote Sensing, Leipzig University, Leipzig, Germany

[3] Institute of Geosciences, University of Potsdam, Potsdam-Golm, Germany

The PIK Atmospheric River Trajectories (PIKART) catalog is a global, high-resolution catalog of atmospheric rivers (ARs). Version 1.1 (v1.1) addresses two algorithmic bugs present in version 1.0 (v1.0): a boundary artifact at 30° E emerging during the extraction of the background component of the integrated vapor transport (IVT), and an error in the AR tracking algorithm that affected the evaluation of genesis and termination at time steps with no overlap between AR shapes and AR trajectories. In addition, v1.1 incorporates several minor corrections and improvements, including a bug fix in the calculation of rank 4 in the AR scale, an extension of the temporal domain to fully cover the years 2024 and 2025, an updated spatial grid aligned with the ECMWF standard, and compatibility with the restructured Copernicus Climate Data Store (CDS). The catalog is available at https://ar.pik-potsdam.de.

PIKART Version 1.1: Release Notes

S. M. Vallejo-Bernal[1,2], T. Braun[1,2], N. Marwan[1,3], and J. Kurths[1]

[1]Research Department Complexity Science, Potsdam Institute for Climate Impact Research (PIK), Member of the Leibniz Association, Potsdam, Germany
[2]Institute for Earth System Science & Remote Sensing, Leipzig University, Leipzig, Germany
[3]Institute of Geoscience, University of Potsdam, Potsdam, Germany

June 12, 2026

Abstract

The PIK Atmospheric River Trajectories (PIKART) catalog [Vallejo-Bernal et al., 2025] is a global, high-resolution catalog of atmospheric rivers (ARs). Version 1.1 (v1.1) addresses two algorithmic bugs present in version 1.0 (v1.0): a boundary artifact at 30° E emerging during the extraction of the background component of the integrated vapor transport (IVT), and an error in the AR tracking algorithm that affected the evaluation of genesis and termination at time steps with no overlap between AR shapes and AR trajectories. In addition, v1.1 incorporates several minor corrections and improvements, including a bug fix in the calculation of rank 4 in the AR scale, an extension of the temporal domain to fully cover the years 2024 and 2025, an updated spatial grid aligned with the ECMWF standard, and compatibility with the restructured Copernicus Climate Data Store (CDS). The catalog is available at `https://ar.pik-potsdam.de`.

1 Introduction

The PIK Atmospheric River Trajectories (PIKART) catalog [Vallejo-Bernal et al., 2025] is a global, comprehensive compilation of atmospheric rivers (ARs), produced at high spatiotemporal resolution from reanalysis data. Building on the image-processing-based IPART-1 detection scheme [Xu et al., 2020], PIKART identifies ARs in an unsupervised fashion by exploiting endogenous synoptic-scale integrated vapor transport (IVT) variability. The tracking algorithm prioritizes large and intense AR features and permits physically sound temporal gaps, thereby improving the representation of long-lived AR trajectories. The catalog provides a broad suite of secondary AR properties, including AR strength ranks, land-intersecting coordinates, and a novel inland penetration index. PIKART is available in both Eulerian and Lagrangian representations and is currently compiled from ERA5 and MERRA-2 reanalysis data [Hersbach et al., 2020, Rienecker et al., 2011]. The ERA5-based version provides a spatiotemporal resolution of 0.5° and 6 hours and is used for all figures, tables, and statistics presented in this document.

After the release of version 1.0 (v1.0), two software bugs were identified: a boundary artifact at 30° E and an error in the AR tracking algorithm affecting the evaluation of genesis and termination when no overlap existed between AR shapes and trajectories. Correcting these issues motivates the release of version 1.1 (v1.1). In addition to these bug fixes, several minor corrections and technical improvements were implemented including a bug fix in the calculation of rank 4 in the AR scale, an extension of the temporal domain to fully include the years 2024 and 2025, an updated spatial grid aligned with the ECMWF standard, and compatibility with the restructured Copernicus Climate Data Store (CDS). This document describes all changes between v1.0 and v1.1 in detail, along with updated catalog statistics.

2 Changes from v1.0 to v1.1 of the PIKART catalog

2.1 Bug fix: Boundary artifact at 30° E in the extraction of the background IVT component

Description. PIKART detects ARs by decomposing the IVT field into a background IVT component and a transient IVT anomaly component (see Section 2.2 in Vallejo-Bernal et al. [2025] for details). In v1.0, this decomposition was performed with the IVT field centered at 210° E by first eroding the image and then applying a morphological

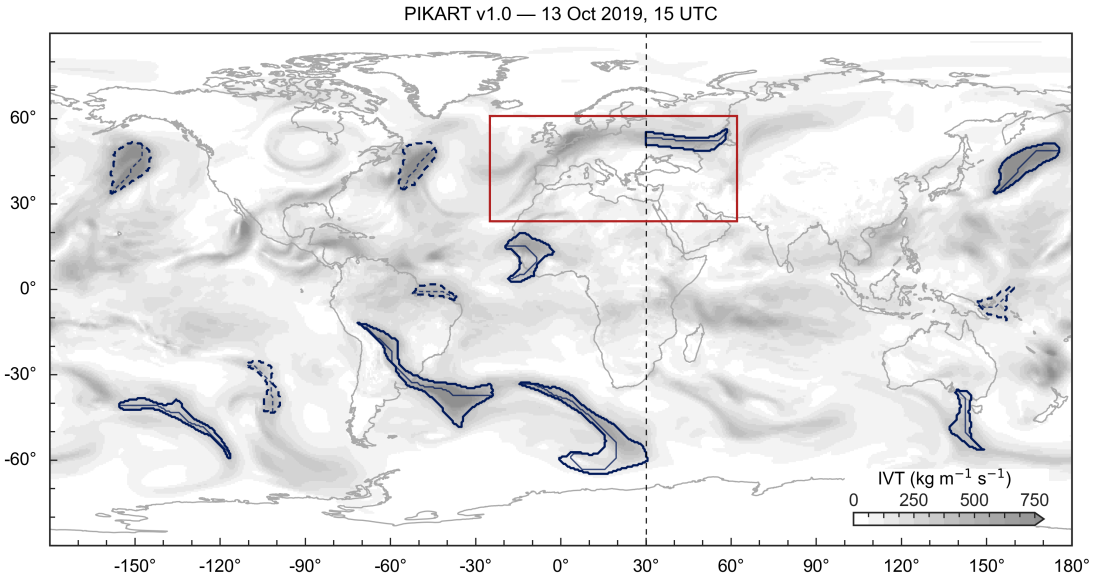

Figure 1: Boundary artifact in v1.0 of the PIKART catalog. The red box indicates a truncated AR contour detected at 30° E, corresponding to the meridional boundary introduced by centering the IVT field at 210° E. Solid and dashed contours denote AR shapes and relaxed AR shapes, respectively, as defined in Subsection 2.3 of Vallejo-Bernal et al. [2025].

reconstruction by dilation using the Python package `scikit-image`. Although the command `skimage.morphology.reconstruction()` successfully extracted the background component of the IVT field, it also introduced a spurious boundary artifact by detecting truncated AR contours at 30° E (Fig. 1), corresponding to the meridional boundary introduced by centering the IVT field at 210° E. These truncated contours generated artificial AR detections, distorted AR geometry near 30° E, and ultimately introduced a discontinuity in AR frequency over Europe (Fig. 4a).

We attempted to resolve this issue by centering the IVT field at different longitudes (e.g. 0° E, 30° E, 90° E, and 270° E), but this only shifted the boundary artifact to the corresponding meridional boundary instead of eliminating it (Fig. 2a,b). Padding the image on both ends to extend the spatial domain before the reconstruction also failed to resolve the issue. After scrutinizing both the documentation and the source code of `scikit-image`, and after attempting to implement the morphological reconstruction by dilation ourselves, we learned that this image-processing task is computationally very demanding. The artifact likely originates from an optimization technique used in the `scikit-image` implementation.

The morphological reconstruction by dilation of the IVT field is the bottleneck in the compilation of the PIKART catalog, and the `scikit-image` package provides an efficient implementation of this operation. Therefore, we continue using it in v1.1, while applying an additional correction to remove the boundary artifact.

Correction. To eliminate the boundary artifact, v1.1 performs two independent extractions of the background component of the IVT field using input data centered at 30° E and 210° E, respectively. Two transient IVT anomaly fields are then computed: $IVT_{\text{anom},30°E}$ (Fig. 2a) and $IVT_{\text{anom},210°E}$ (Fig. 2b). Lastly, the transient IVT anomaly is defined as the gridpoint-wise minimum of the two fields: $IVT_{\text{anom}} = \min\left(IVT_{\text{anom},30°E}, IVT_{\text{anom},210°E}\right)$.

This procedure ensures that artifacts generated at the boundary of either reconstruction are suppressed by the unaffected counterpart (Fig. 2c). The correction fully removes the truncated AR detections at the meridional boundary (Fig. 3) and eliminates the discontinuity in AR frequency over Europe (Fig. 4b), while preserving the computational efficiency of the original morphological reconstruction by dilation workflow. Implementation required the creation or modification of the following scripts:

```
05_CDO_shift_longitude_ERA5.sh
06_check_grid_input_data.py
07a_IVT_top_hat_reconstruction_30E.py
07b_IVT_top_hat_reconstruction_210E.py
08_CDO_min_anomaly.sh
submit_07a.sh
submit_07b.sh
```

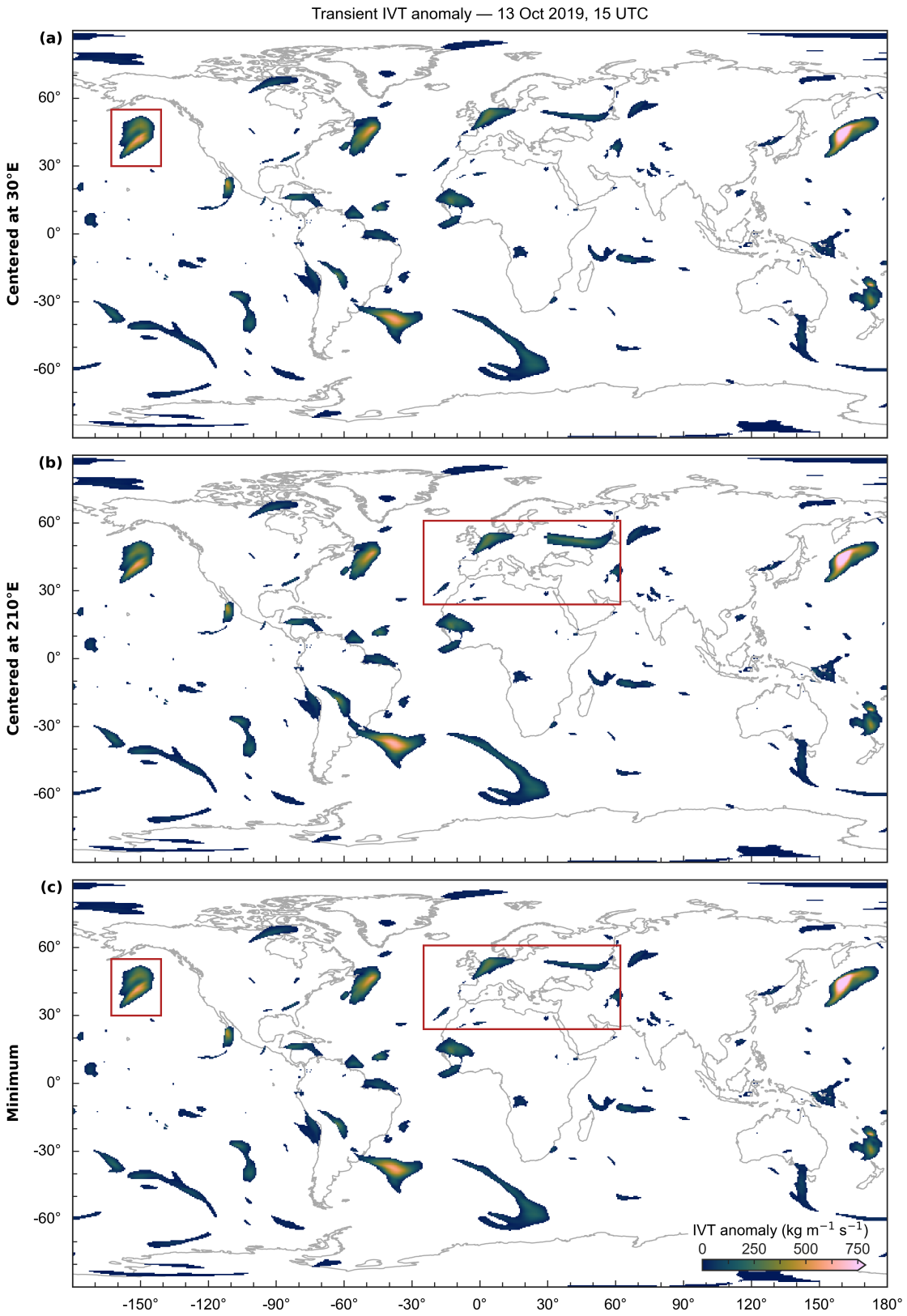

Figure 2: Transient IVT anomaly fields calculated from IVT fields centered at (a) 30° E and (b) 210° E. In both cases, artifacts remain visible at the corresponding meridional boundary (red boxes). Panel (c) shows the transient IVT anomaly obtained from the gridpoint-wise minimum of (a) and (b), which suppresses the boundary artifacts.

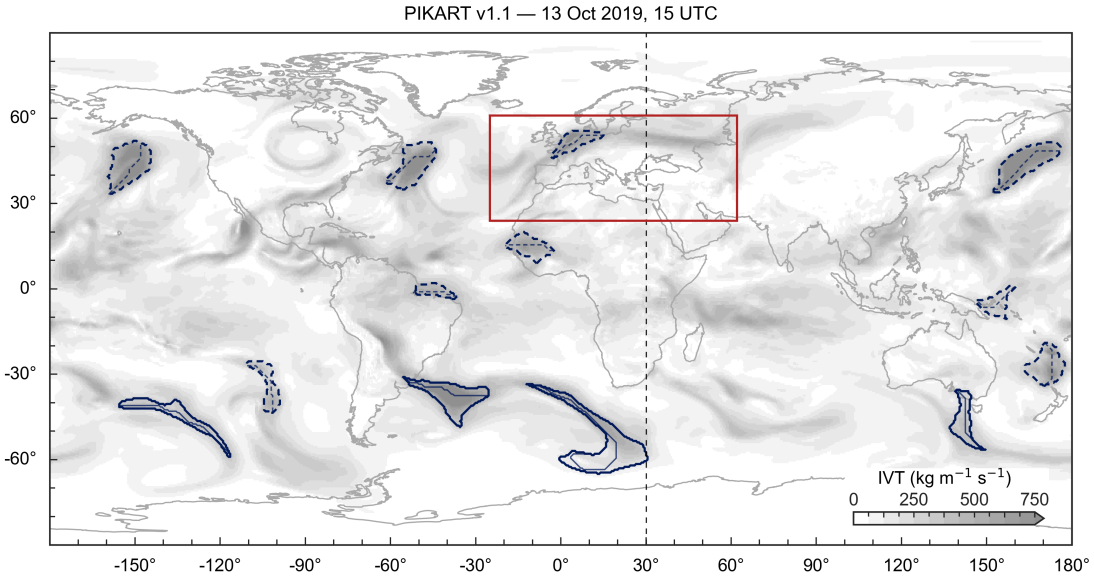

Figure 3: AR detection in v1.1 of the PIKART catalog. The truncated AR contour detected at 30° E in v1.0 is no longer present and is replaced by a relaxed AR shape located at approximately 5° E. Note that the IVT plume transiting Europe is detected as two separated transient IVT anomalies (Fig. 2), from which only the westernmost feature is cataloged as an AR after tracking and post-processing in the PIKART v1.1 algorithm. Solid and dashed contours as in Fig. 1.

2.2 Bug fix: Genesis and termination in the AR tracking algorithm

Description. PIKART tracks AR trajectories by evaluating overlaps between AR shapes identified at time t and AR trajectories tracked up to times $t-1$ and $t-2$ (see Section 2.4 in Vallejo-Bernal et al. [2025] for details). In v1.0 of the PIKART tracking algorithm, genesis and termination were only evaluated when at least one overlap existed between AR shapes and AR trajectories. This approach was erroneous, since genesis and termination events may occur precisely when no overlap is present. As a result, AR trajectories that should have terminated could be erroneously extended, while newly emerging AR trajectories could fail to initiate, leading to incorrect trajectory bookkeeping at time steps with no detected ARs or no overlaps.

Correction. In v1.1, genesis and termination are evaluated at every time step, independent of whether spatial overlap between AR shapes and trajectories exists. This ensures consistent lifecycle bookkeeping across the full temporal domain, including intervals with no active ARs. The correction was implemented in:

```
13_AR_tracking.py
```

2.3 Minor corrections and technical improvements

The following additional changes were introduced in v1.1 of the PIKART catalog:

1. **Updated ERA5 download and IVT calculation scripts.** Following the migration of the Copernicus Climate Data Store (CDS) to a new platform, scripts

   ```
   00_CDS_download_ERA5.py
   01_calculate_IVT_ERA5.py
   ```

   were updated to ensure compatibility with the new data infrastructure. Since the `.nc` format remains experimental, ERA5 reanalysis data are now downloaded in `.grib` format. For the calculation of the IVT fields, ERA5 input data are now read using the `cfgrib` engine, and the pressure-level variable was updated from `level` to `isobaricInhPa`.

2. **Updated spatial grid.** PIKART v1.1 uses the standard spatial grid of the European Centre for Medium-Range Weather Forecasts (ECMWF), replacing the custom grid used in v1.0. The new grid was implemented in script

   ```
   03_CDO_regridding_ERA5.sh
   ```

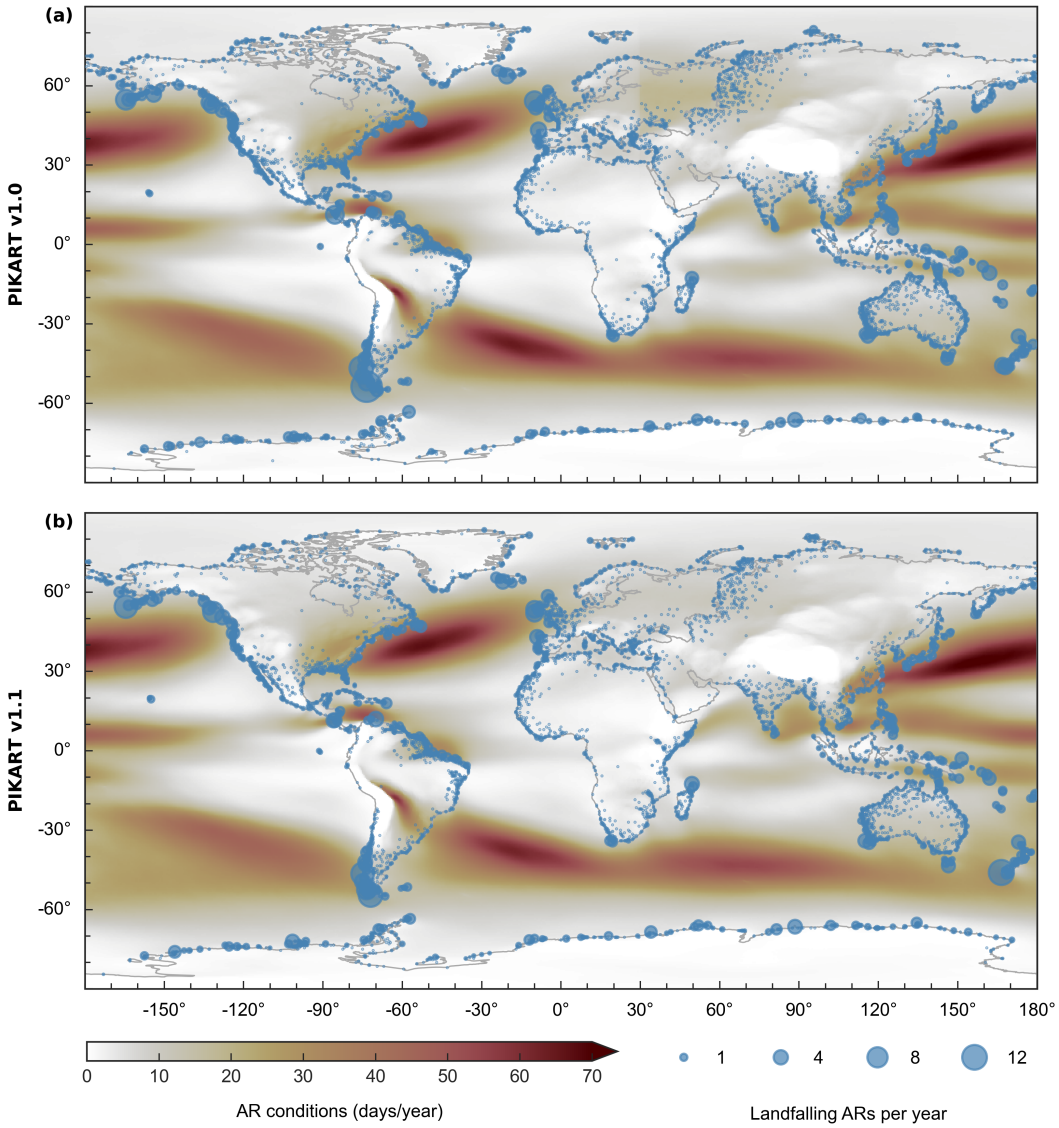

Figure 4: Global AR frequency from 1979 to 2023 for (a) PIKART v1.0 and (b) PIKART v1.1. The shading indicates the average fraction of time a location is exposed to AR conditions, and bubbles indicate the mean annual number of landfalling ARs. The spurious enhancement near 30° E in v1.0, caused by the boundary artifact arising during the morphological reconstruction by dilation of the IVT field, is absent in v1.1.

The continental and insular land-sea masks used for land-intersection classification are now also provided on the ECMWF standard grid.

3. **Updated longitude-shifting workflow.** In v1.0, script `05_CDO_shift_longitude_ERA5.sh` shifted the longitude of IVT_u, IVT_v, and IVT from [0° E, 360° E] to [−180° E, 180° E], and the longitude of the IVT magnitude from [0° E, 360° E] to [30° E, 390° E].
   In v1.1, the longitude of IVT_u, IVT_v, and IVT is shifted from [0° E, 360° E] to [−180° E, 180° E] in script

```
04_CDO_6hr_ERA5.sh
```

   while script

```
05_CDO_shift_IVT_longitude_ERA5.sh
```

   prepares two shifted IVT fields for the morphological top-hat reconstruction: one centered at 30° E and another centered at 210° E.

In the new configuration file `config_PIKART_V1.1.yml`, the variable `ivt_shift_folder` was replaced by the variables `ivt_210E_folder` and `ivt_30E_folder`.

4. **Improved handling of temporal-domain boundaries.** In v1.0 of the PIKART catalog, the initial and final years of the record period (1940 and 2023) were missing the first and last 32 time steps, respectively, due to insufficient data to construct the synoptic spatiotemporal neighborhood required by the AR detection algorithm. In v1.1, this issue was corrected in scripts

```
07a_IVT_top_hat_reconstruction_30E.py
07b_IVT_top_hat_reconstruction_210E.py
```

The algorithm now attempts to load IVT data from the years preceding and following the cataloged period. If the required data from either year are unavailable in the input folders `ivt_210E_folder` and `ivt_30E_folder`, the corresponding end of the temporal domain is padded with fields filled with NaN values. As a result, both the initial and final years are now fully cataloged in v1.1.

5. **Grid matching in land-intersection script.** In v1.0, the script

```
18_PIKART_land_intersection.py
```

loaded the land-sea masks for continental and insular landmasses only after reversing the latitude axis. In v1.1, the script attempts to match the grids of PIKART and the land-sea masks both with and without reversing the latitude axis. If the grids do not match after both attempts, the script exits with an informative error message, preventing silent failures.

6. **Bug fix in the AR scale calculation.** In v1.0, rank 4 of the AR scale was incorrectly calculated because the upper bound of the IVT intensity was set to 1200 $\mathrm{kg\,m^{-1}\,s^{-1}}$ instead of 1250 $\mathrm{kg\,m^{-1}\,s^{-1}}$. In v1.1, this typo was corrected in the script

```
ardt_functions.py
```

In addition, the calculation of rank 5 was simplified.

3 Impact on catalog statistics

Table 1 provides a direct comparison of key statistics between v1.0 and v1.1. The reported values correspond to the same variables listed in Table 1 of the original manuscript [Vallejo-Bernal et al., 2025]. The first two columns compare v1.0 and v1.1 over the same cataloged period (1940–2023), while the third column reports the statistics of v1.1 for the extended period 1940–2025. Figure 5 presents the updated workflow used to compile PIKART v1.1.

Table 1: Comparison of PIKART catalog statistics between v1.0 and v1.1.

	PIKART v1.0	**PIKART v1.1**	**PIKART v1.1**
Reanalysis	ERA5	ERA5	ERA5
Temporal domain	1940–2023	1940–2023	1940–2025
Spatial extent	Global	Global	Global
Temporal resolution (hr)	6	6	6
Spatial resolution (°)	0.50×0.50	0.50×0.50	0.50×0.50
AR trajectories	134.693	134.473	137.592
Landfalling ARs	41.150	41.252	41.858
Inland penetrating ARs	9.697	9.577	9.665
IVT median ($\mathrm{kg\,m^{-1}\,s^{-1}}$)	447.30	448.04	448.77
IVT 95th percentile ($\mathrm{kg\,m^{-1}\,s^{-1}}$)	619.37	619.19	620.43
Duration median (d)	1.75	1.5	1.5
Duration 95th percentile (d)	8.25	8.25	8.25
Mean NH latitude (°N)	46.11	45.98	45.99
Mean SH latitude (°S)	44.07	44.07	44.09

NH: Northern Hemisphere. SH: Southern Hemisphere.

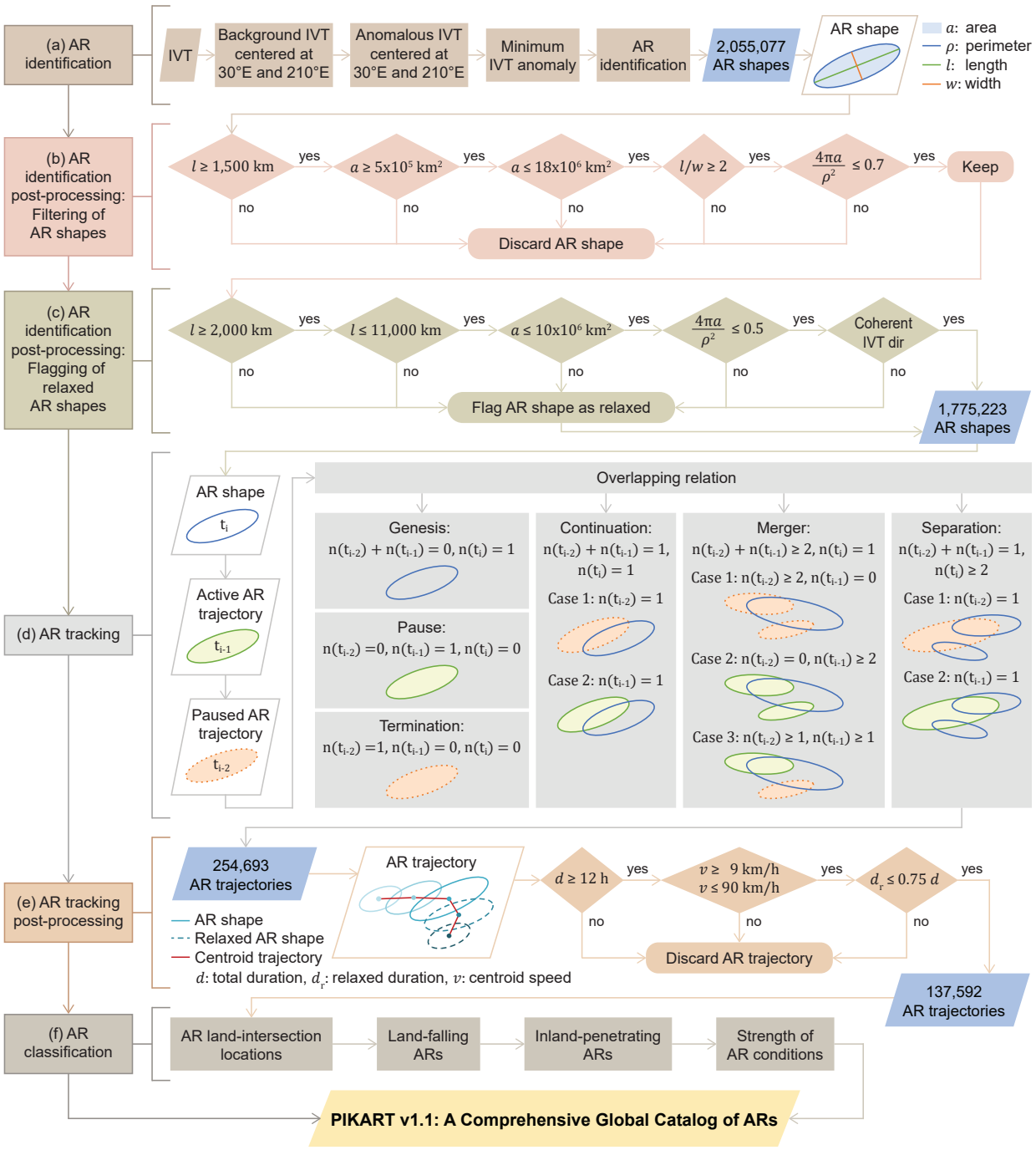

Figure 5: Workflow for compiling v1.1 of the PIKART catalog of ARs. The figure illustrates the updated detection algorithm together with the tracking and post-processing stages, following the structure of Fig. 1 in the original manuscript [Vallejo-Bernal et al., 2025]. The reported numbers of AR shapes and trajectories correspond to PIKART v1.1 compiled using ERA5 data from 1940 to 2025.

4 Recommendations

Users working with v1.0 are encouraged to transition to v1.1, particularly for analyses involving AR activity near 30° E, AR genesis and termination statistics, or the AR scale. Users should cite the original PIKART paper [Vallejo-Bernal et al., 2025] and may additionally cite the present release notes when using v1.1 data.

5 Data availability

PIKART v1.1 data and algorithm are freely available at `https://ar.pik-potsdam.de` and `https://zenodo.org/records/17109482`, respectively. The ERA5 reanalysis datasets are freely available through the Copernicus Climate Data Store via `https://doi.org/10.24381/cds.bd0915c6` [Hersbach et al., 2023a] and `https://doi.org/10.24381/cds.adbb2d47` [Hersbach et al., 2023b].

Acknowledgements

The PIKART catalog is compiled on the high-performance computing system *Foote* at the Potsdam Institute for Climate Impact Research, which is supported by the Ministry of Research, Science and Culture (MWFK) of the State of Brandenburg, Germany (Grant No. 22-Z105-05/002/001). TB acknowledges support from the European Space Agency (ESA) Living Planet Fellowship through the *ARNETLAB* project (4000144018/24/I-DT-lr).

References

Hans Hersbach, Bill Bell, Paul Berrisford, Shoji Hirahara, András Horányi, Joaquín Muñoz-Sabater, Julien Nicolas, Carole Peubey, Raluca Radu, Dinand Schepers, Adrian Simmons, Cornel Soci, Saleh Abdalla, Xavier Abellan, Gianpaolo Balsamo, Peter Bechtold, Gionata Biavati, Jean Bidlot, Massimo Bonavita, Giovanna De Chiara, Per Dahlgren, Dick Dee, Michail Diamantakis, Rossana Dragani, Johannes Flemming, Richard Forbes, Manuel Fuentes, Alan Geer, Leo Haimberger, Sean Healy, Robin J. Hogan, Elías Hólm, Marta Janisková, Sarah Keeley, Patrick Laloyaux, Philippe Lopez, Cristina Lupu, Gabor Radnoti, Patricia de Rosnay, Iryna Rozum, Freja Vamborg, Sebastien Villaume, and Jean-Noël Thépaut. The ERA5 global reanalysis. *Quarterly Journal of the Royal Meteorological Society*, 146(730):1999–2049, 2020. doi: https://doi.org/10.1002/qj.3803.

Hans Hersbach, Bill Bell, Paul Berrisford, Gionata Biavati, András Horányi, Joaquín Muñoz-Sabater, Julien Nicolas, Carole Peubey, Raluca Radu, Iryna Rozum, Dinand Schepers, Adrian Simmons, Cornel Soci, Dick Dee, and Jean-Noël Thépaut. ERA5 hourly data on pressure levels from 1940 to present. *Copernicus Climate Change Service (C3S) Climate Data Store (CDS) [data set]*, 2023a. doi: https://doi.org/10.24381/cds.bd0915c6.

Hans Hersbach, Bill Bell, Paul Berrisford, Gionata Biavati, András Horányi, Joaquín Muñoz-Sabater, Julien Nicolas, Carole Peubey, Raluca Radu, Iryna Rozum, Dinand Schepers, Adrian Simmons, Cornel Soci, Dick Dee, and Jean-Noël Thépaut. ERA5 hourly data on single levels from 1940 to present. *Copernicus Climate Change Service (C3S) Climate Data Store (CDS) [data set]*, 2023b. doi: https://doi.org/10.24381/cds.adbb2d47.

Michele M. Rienecker, Max J. Suarez, Ronald Gelaro, Ricardo Todling, Julio Bacmeister, Emily Liu, Michael G. Bosilovich, Siegfried D. Schubert, Lawrence Takacs, Gi-Kong Kim, Stephen Bloom, Junye Chen, Douglas Collins, Austin Conaty, Arlindo da Silva, Wei Gu, Joanna Joiner, Randal D. Koster, Robert Lucchesi, Andrea Molod, Tommy Owens, Steven Pawson, Philip Pegion, Christopher R. Redder, Rolf Reichle, Franklin R. Robertson, Albert G. Ruddick, Meta Sienkiewicz, and Jack Woollen. MERRA: NASA's Modern-Era Retrospective Analysis for Research and Applications. *Journal of Climate*, 24(14):3624 – 3648, 2011. doi: https://doi.org/10.1175/JCLI-D-11-00015.1.

S. M. Vallejo-Bernal, T. Braun, N. Marwan, and J. Kurths. PIKART: A comprehensive global catalog of atmospheric rivers. *Journal of Geophysical Research: Atmospheres*, 130(15):e2024JD041869, 2025. doi: https://doi.org/10.1029/2024JD041869.

G. Xu, C. Ma, P. Chang, and L. Wang. Image-processing-based atmospheric river tracking method version 1 (IPART-1). *Geoscientific Model Development*, 13(10):4639–4662, 2020. doi: https://doi.org/10.5194/gmd-13-4639-2020.